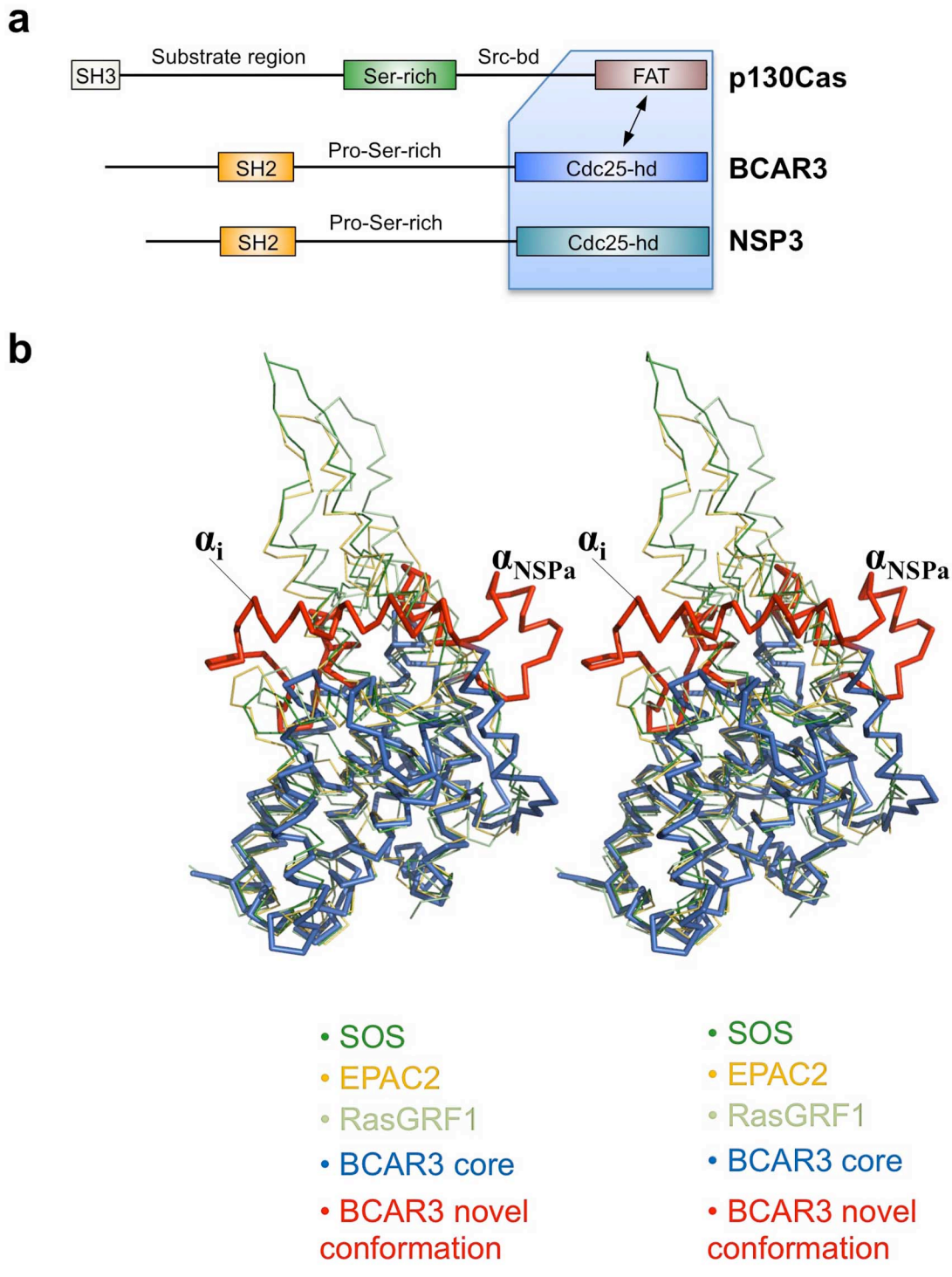

Supplementary Figure 1. NSP and Cas domain organization and comparison of the BCAR3 Cdc25-homology domain structure with those of SOS, EPAC and RasGRF1. **(a)** Schematic domain organizations of p130Cas, BCAR3 and NSP3. p130Cas consists of an N-terminal Src-homology 3 (SH3) domain followed by a Tyrosine-rich "Substrate region", a defined Serine-rich domain (Ser-rich), a Src-binding "domain" (Src-bd) and a predicted focal adhesion targeting domain (FAT) at its C-terminus. Although they differ in the length of their N-terminal extension, both BCAR3 and NSP3 contain a Src-homology 2 (SH2) domain preceding a proline and serine rich region (Pro-Ser-rich) and a predicted C-terminal Cdc25-homology domain (Cdc25-hd). The NSP-Cas interaction is mediated by their respective C-terminal domains (Cdc25-hd and FAT respectively; blue background). Folded domains are indicated by boxes. Displayed arrangements are typical of all NSP and Cas family members. **(b)** Stereo representation of the Cα-trace of BCAR3 (thick trace in blue/red) superimposed on the structures of the Cdc25-homology domains (thin traces) of SOS (dark green; PDBid: 1bkd), EPAC2 (yellow; PDBid: 3cf6), and RasGRF1 (pale green, PDBid: 2ije). The core of the BCAR3 Cdc25-homology domain (blue) overlays well with the other Cdc25-homology domains, however in BCAR3 elements that are key for GEF function are grossly distorted and adopt a novel conformation (red).

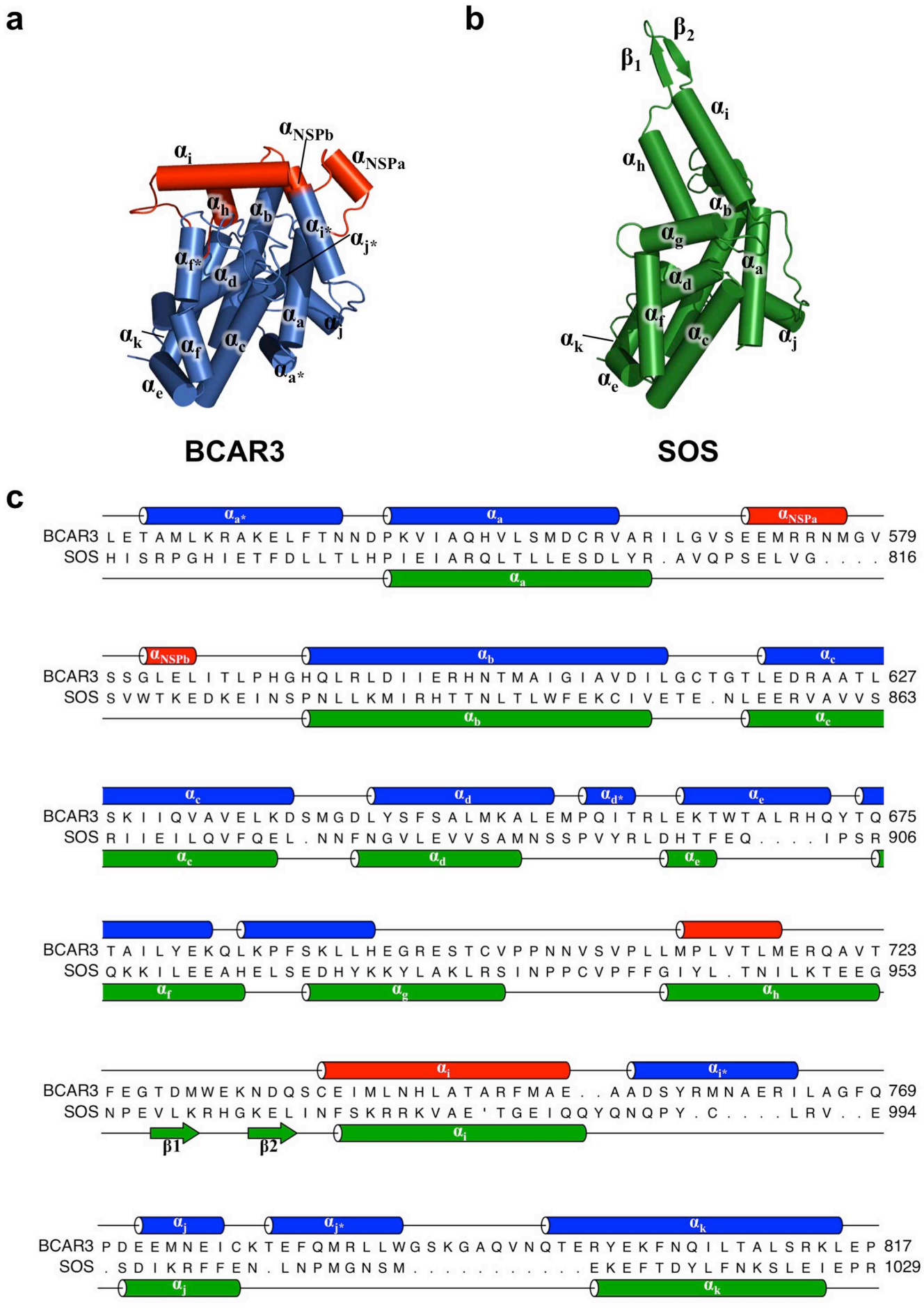
a
b
BCAR3
SOS
c
BCAR3 L E T A M L K R A K E L F T N N D P K V I A Q H V L S M D C R V A R I L G V S E E M R R N M G V 579
SOS H I S R P G H I E T F D L L T L H P I E I A R Q L T L L E S D L Y R . A V Q P S E L V G 816
BCAR3 S S G L E L I T L P H G H Q L R L D I I E R H N T M A I G I A V D I L G C T G T L E D R A A T L 627
SOS S V W T K E D K E I N S P N L L K M I R H T T N L T L W F E K C I V E T E . N L E E R V A V V S 863
BCAR3 S K I I Q V A V E L K D S M G D L Y S F S A L M K A L E M P Q I T R L E K T W T A L R H Q Y T Q 675
SOS R I I E I L Q V F Q E L . N N F N G V L E V V S A M N S S P V Y R L D H T F E Q . . . . I P S R 906
BCAR3 T A I L Y E K Q L K P F S K L L H E G R E S T C V P P N N V S V P L L M P L V T L M E R Q A V T 723
SOS Q K K I L E E A H E L S E D H Y K K Y L A K L R S I N P P C V P F F G I Y L . T N I L K T E E G 953
BCAR3 F E G T D M W E K N D Q S C E I M L N H L A T A R F M A E . . A A D S Y R M N A E R I L A G F Q 769
SOS N P E V L K R H G K E L I N F S K R R K V A E ' T G E I Q Q Y Q N Q P Y . C . . . . L R V . . E 994
BCAR3 P D E E M N E I C K T E F Q M R L L W G S K G A Q V N Q T E R Y E K F N Q I L T A L S R K L E P 817
SOS . S D I K R F F E N . L N P M G N S M . . . . . E K E F T D Y L F N K S L E I E P R 1029

Supplementary Figure 2. Secondary Structure of BCAR3 compared to SOS. **(a)** The BCAR3 structure with secondary structure annotated. Overall BCAR3 adopts a Cdc25-homology domain fold (blue) but adopts an alternative conformation in critical regions (red). **(b)** The prototypical Cdc25-homology domain from SOS with secondary structure annotated. Displayed is the Cdc25-homology domain of the GTPase exchange factor SOS (son of sevenless, green; pdb entry 1bkd) with annotations as designated in Boriack-Sjodin et al.[30]. **(c)** Structure-based sequence alignment of BCAR3 and SOS. The primary sequences of the two proteins were aligned based on structural overlays. Secondary structure elements are displayed above (blue/red) for BCAR3 and below (green) for SOS. BCAR3 displays two distinctly new helixes (α_{NSPa}, α_{NSPb}, designated NSP specific region and shown in red) and also shows a distinctly different conformation for helices α_h and α_i (red). Further divergent elements found in the NSP Cdc25-homology domain of BCAR3 are depicted with asterisks.

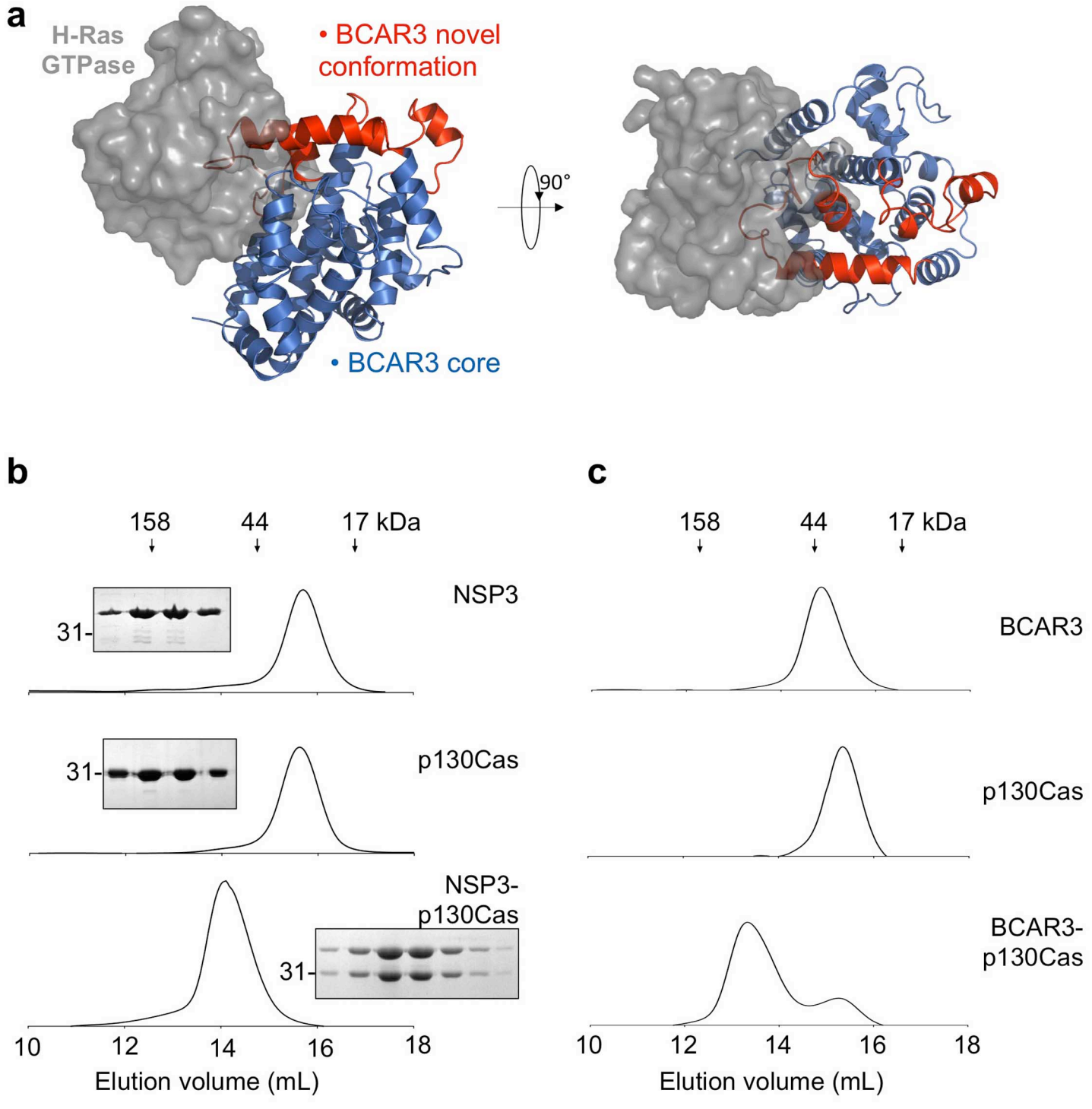

Supplementary Figure 3. Occluded BCAR3 GTPase site and NSP3, BCAR3 and p130Cas gel filtration. **(a)** The BCAR3 Cdc25-homology domain has an occluded Ras GTPase binding site. To generate a hypothetical complex of BCAR3 with a Ras GTPase, the H-Ras-SOS complex (PDBid: 1bkd) was overlaid on BCAR3 and the SOS structure was then removed. The hypothetical complex shows severe steric clashes between BCAR3 and H-Ras (grey, surface representation), demonstrating that the putative GTPase binding site of BCAR3 is occluded. **(b)** Gel filtration analysis of the NSP3 and p130Cas C-terminal domains and their complex. Individual proteins migrate as monomers with profiles indicative of high protein quality (apparent molecular weight of ~ 30 kDa and 31 kDa, compared to expected molecular weights of 36 kDa and 27 kDa respectively) and form a 1:1 complex with an apparent molecular weight of 69 kDa (see also analytical ultracentrifugaion experiments in Figure S7). SDS-PAGEs of peak fractions are also displayed. **(c)** Gel filtration analysis of BCAR3 and p130Cas C-terminal domains and their complex. BCAR3 migrates as a monomer with a profile indicative of high protein quality (apparent molecular weight of ~ 42 kDa, compared to an expected molecular weight of 38 kDa) and forms a 1:1 complex with p130Cas that has an apparent molecular weight of ~87 kDa.

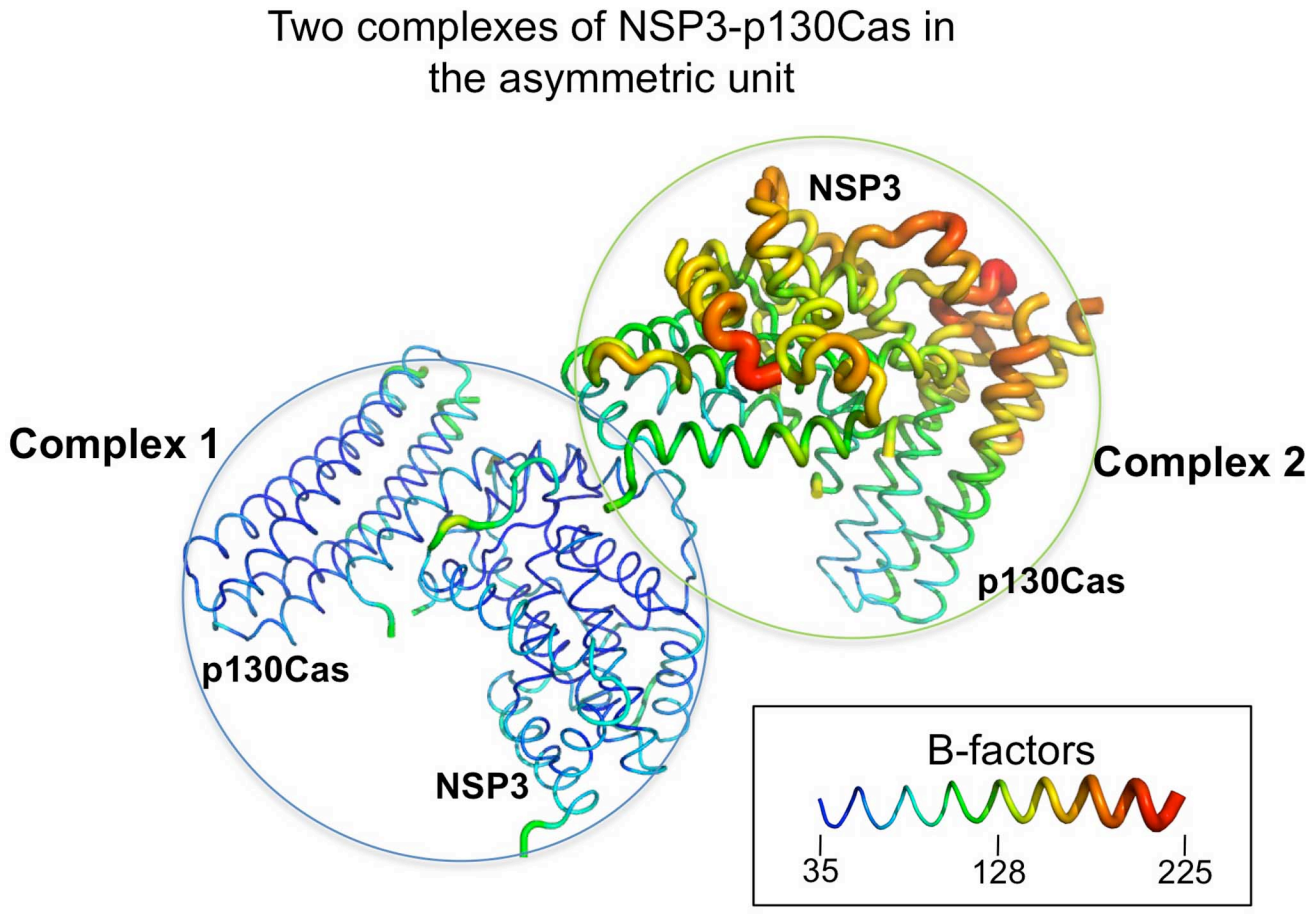

Supplementary Figure 4. The asymmetric unit contains two p130Cas-NSP3 complexes. Displayed are the two complexes present in the asymmetric unit with line color and thickness indicating relative crystallographic B-factors (see key). In line with lower B-factors, complex 1 was more clearly defined by electron density.

Analytical ultra-centrifugation of the NSP3-p130Cas complex at three concentrations

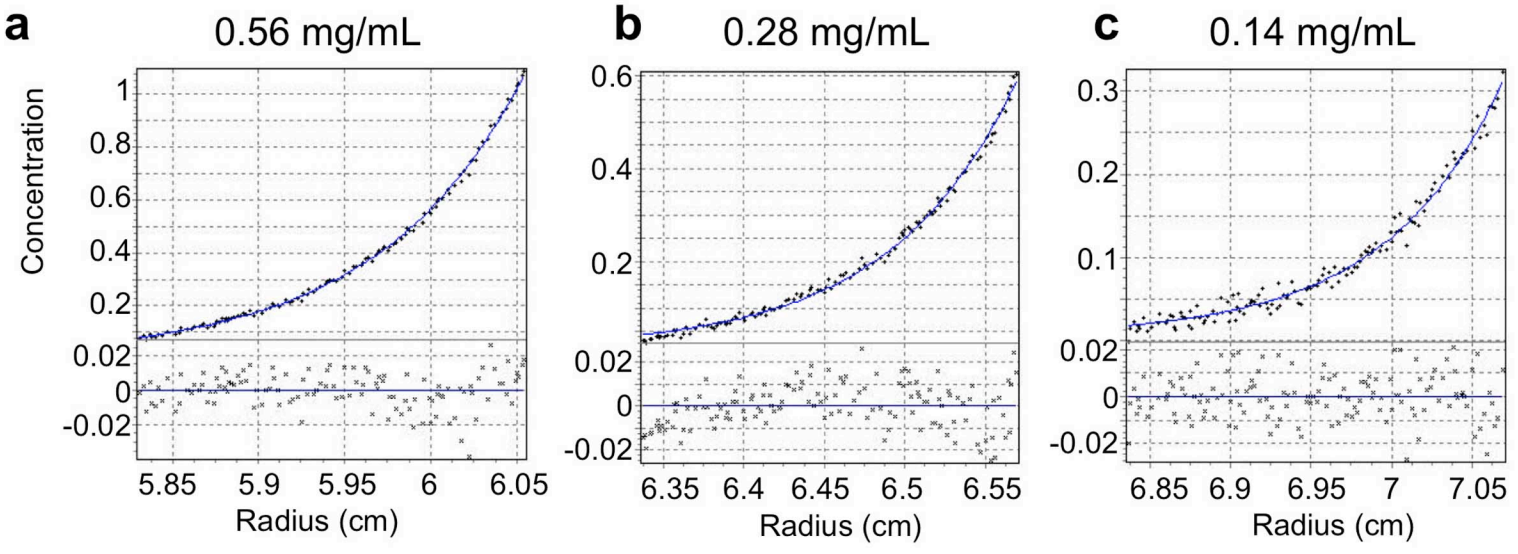

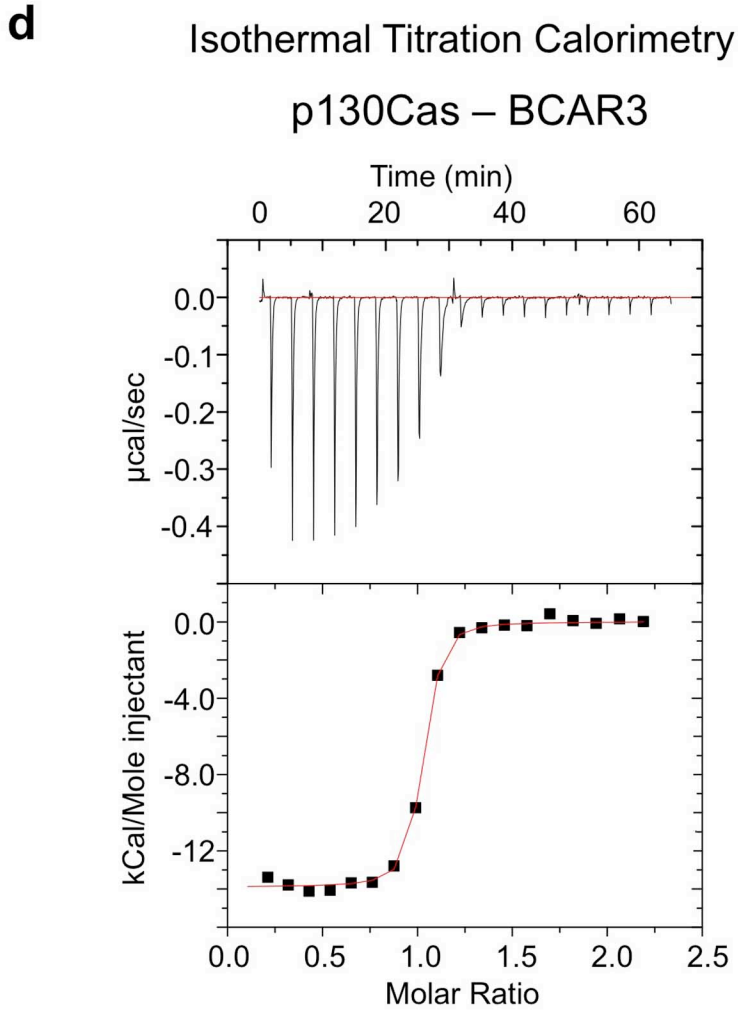

Supplementary Figure 5. AUC and ITC analysis of NSP–Cas complexes. **(a–c)** Analytical ultracentrifugation analysis of the p130Cas-NSP3 complex. The three panels show sedimentation equilibrium measurements of the NSP3-p130Cas complex at concentrations of 0.56 mg/ml **(a)**, 0.28 mg/ml **(b)** and 0.14 mg/ml **(c)**. The data were fitted to a single ideal species model resulting in an average molecular weight of 63.38 kDa, which is within 2% of the calculated molecular weight (62.24 kDa) of a 1:1 NSP3-p130Cas complex. **(d)** Isothermal titration calorimetry analysis of p130Cas binding to NSP3 and BCAR3. Titration of BCAR3 with p130Cas (injected). The calculated dissociation constants for BCAR3 binding to p130Cas indicate a low dissociation constant of 30 nM. NB. Although several titrations suggestive of a strong binding event were performed with NSP3 and p130Cas, a small enthalpic contribution prevented quantitative analysis of this calorimetry data.

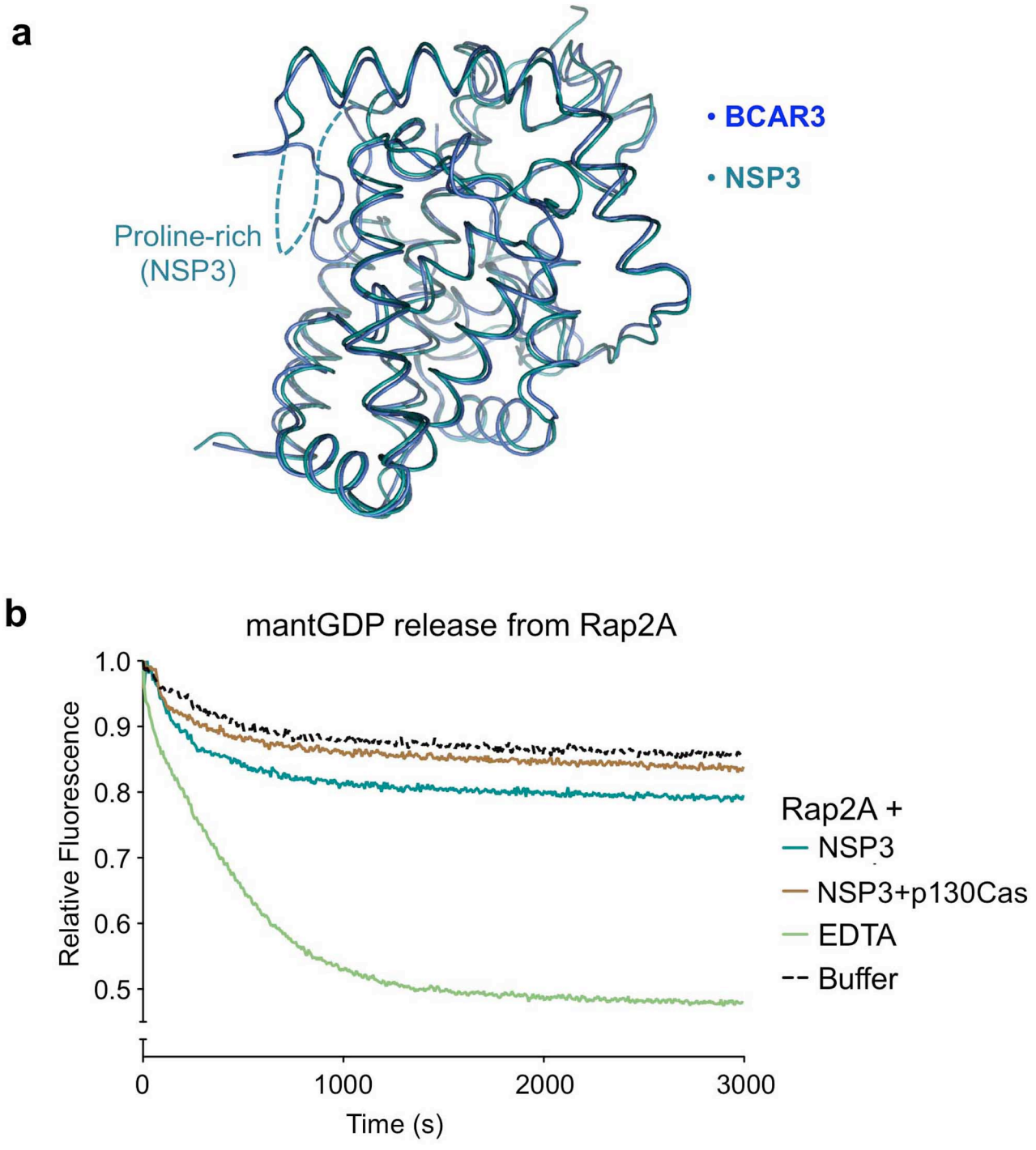

Supplementary Figure 6. Comparison of BCAR3 with NSP3 and NSP3 Rap2A GTPase exchange assay. **(a)** Comparison of the unbound BCAR3 Cdc25-homology domain with the NSP3 Cdc25-homology domain from the NSP3-p130Cas complex. Superposition of backbone representations of BCAR3 (blue) and NSP3 (cyan). The orientation is equivalent to that used in Figures 2–4. Unbound BCAR3 and NSP3 in complex with p130Cas adopt nearly identical conformations, as indicated by an RMSD of 0.97 Å. The proline-rich linker region (residues 599-612) of NSP3 is not defined in the structure and is indicated by a dotted line in the NSP3 model. **(b)** NSP3 does not promote nucleotide exchange in Rap2A in the presence or the absence of p130Cas. Rap2A GTPase was loaded with mant-GDP and then treated with either buffer (negative control), EDTA (positive control), the recombinant NSP3 Cdc25-homology domain, or NSP3 with the p130Cas C-terminal domain. No detectable mant-GDP release was induced by NSP3 alone or together with p130Cas, whereas treatment with EDTA readily induced nucleotide release from Rap2A.

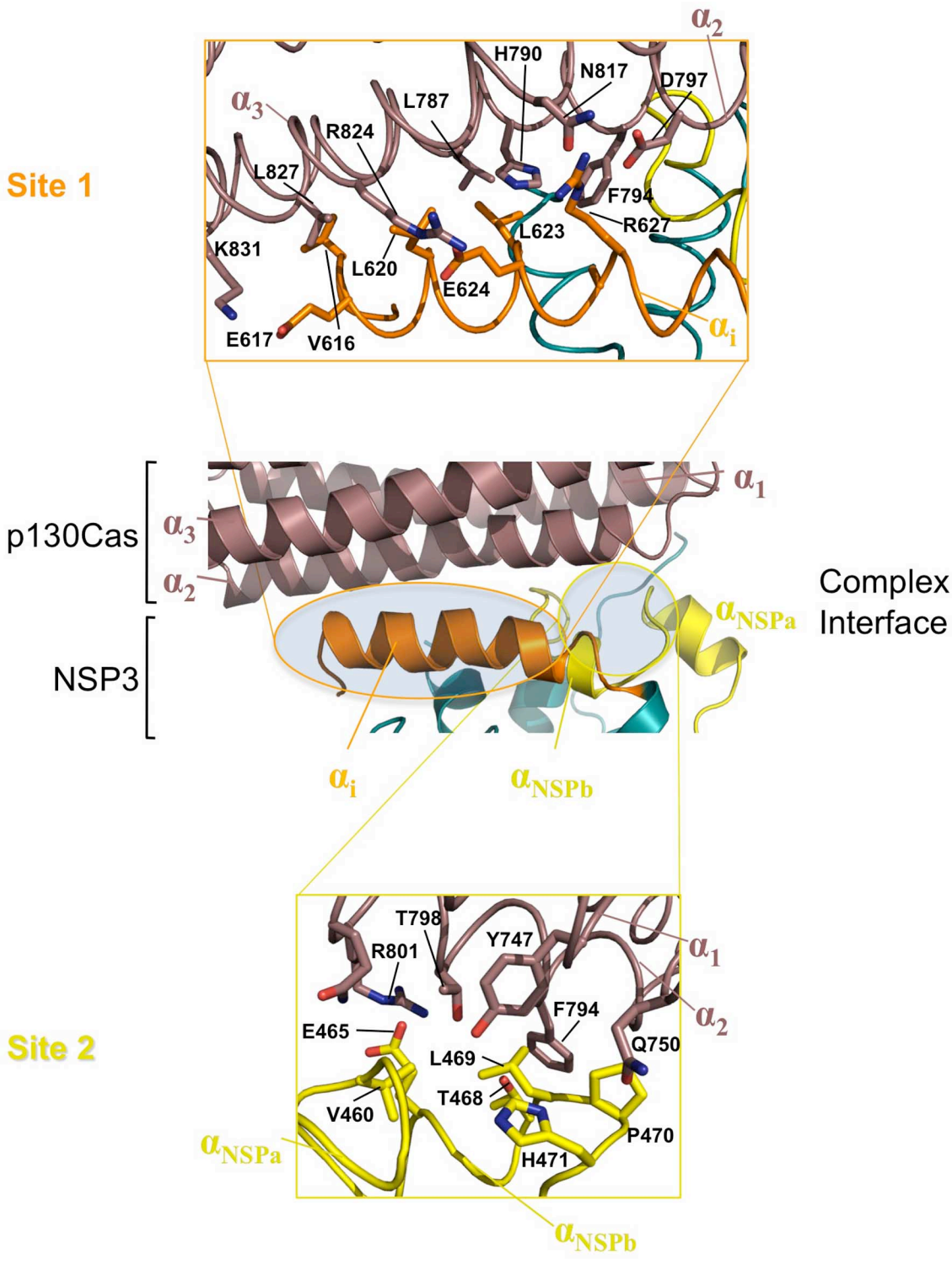

Supplementary Figure 7. The NSP3–p130Cas interface in detail. **(a)** The NSP3 Cdc25-homology domain interaction with the FAT domain of p130Cas is mediated by two main interaction sites. Close up of the complex interface (middle) with detail of Site 1 interaction displayed above and Site 2 interaction displayed below. Structural elements rooted in the closed conformation of NSP3 are providing site 1 and 2 interaction residues and colored orange and yellow respectively. Secondary structure elements of both NSP3 and p130Cas (brown) are annotated.

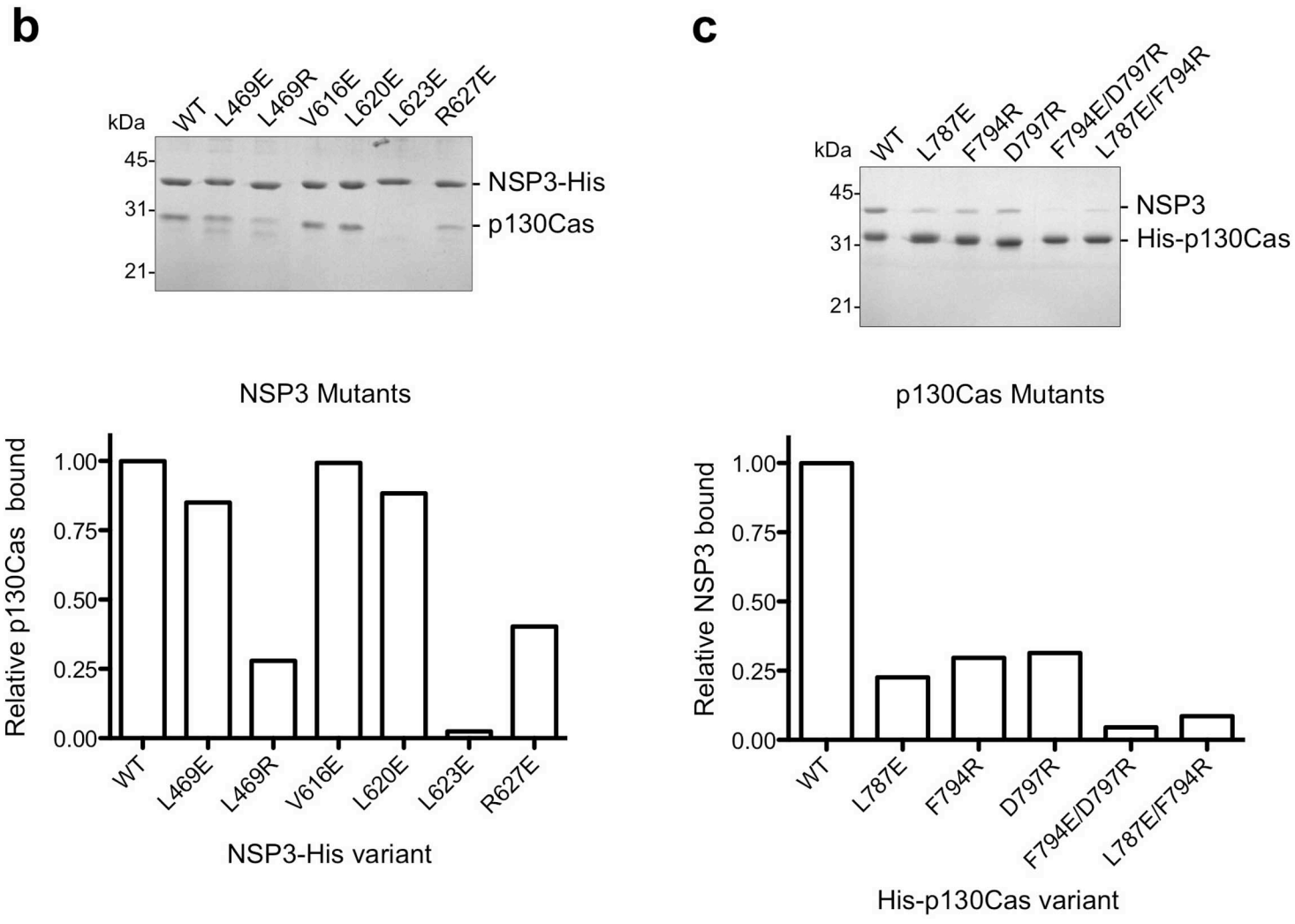

Supplementary Figure 7. continued. Densitometry analysis of NSP3-p130Cas interaction*s in vitro*. Panels **b** and **c** correspond to panels in main **Fig. 4b** and **e** respectively**. (b)** The ratio of untagged p130Cas bound to His-tagged NSP3 was calculated for each lane and is expressed as a relative ratio compared to the proportion of wild-type p130Cas bound by wild-type NSP3. **(c)** Corresponding analysis of p130Cas mutants binding to wild-type NSP3.

a

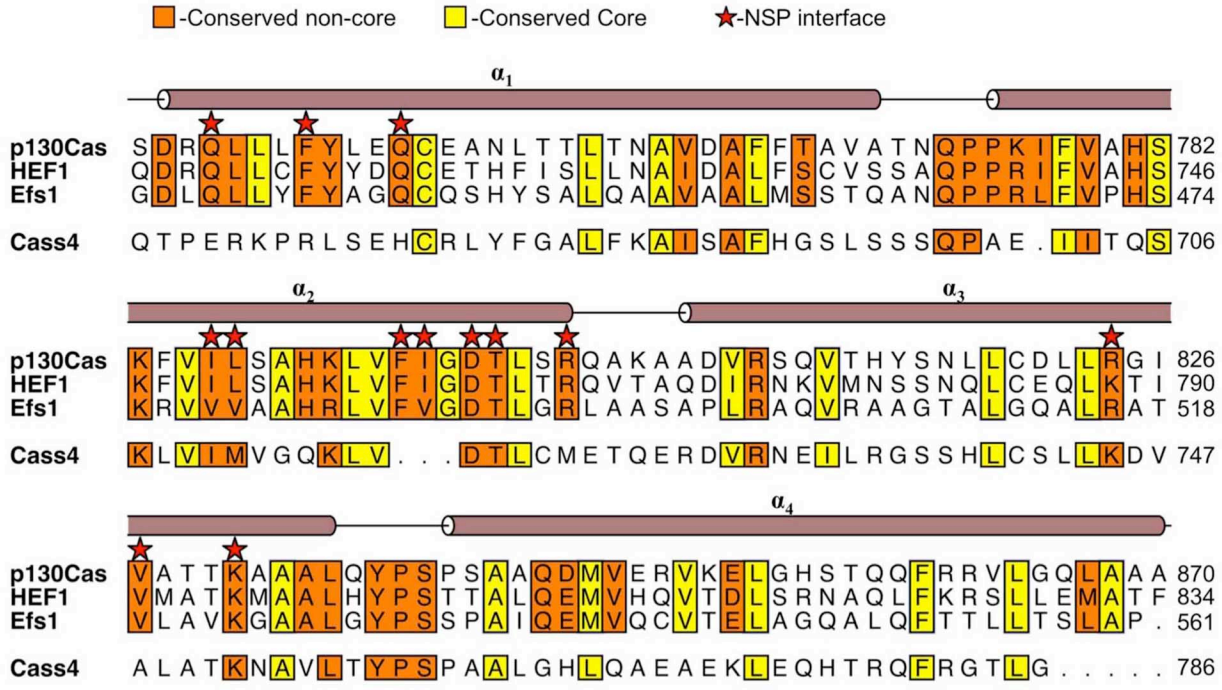

Supplementary Figure 8. Conservation of NSP–Cas binding interfaces. **(a)** Conservation of NSP-binding residues in Cas-family FAT domains. Sequence alignment of the C-terminal domains of p130Cas, Hef1, Efs1, and the more divergent CASS4. Secondary structure elements of the p130Cas FAT domain derived from the p130Cas-NSP3 complex structure are indicated. Conserved residues participating in the hydrophobic core of the p130Cas four-helix bundle are indicated by a yellow background while conserved non-core residues have an orange background. Key residues for Cas-NSP interactions (identified in the NSP3-p130Cas complex structure and schematically shown in **Fig. 4a**) are indicated with red stars. The more divergent CASS4 protein was omitted from initial conservation assignment and colored manually.

b

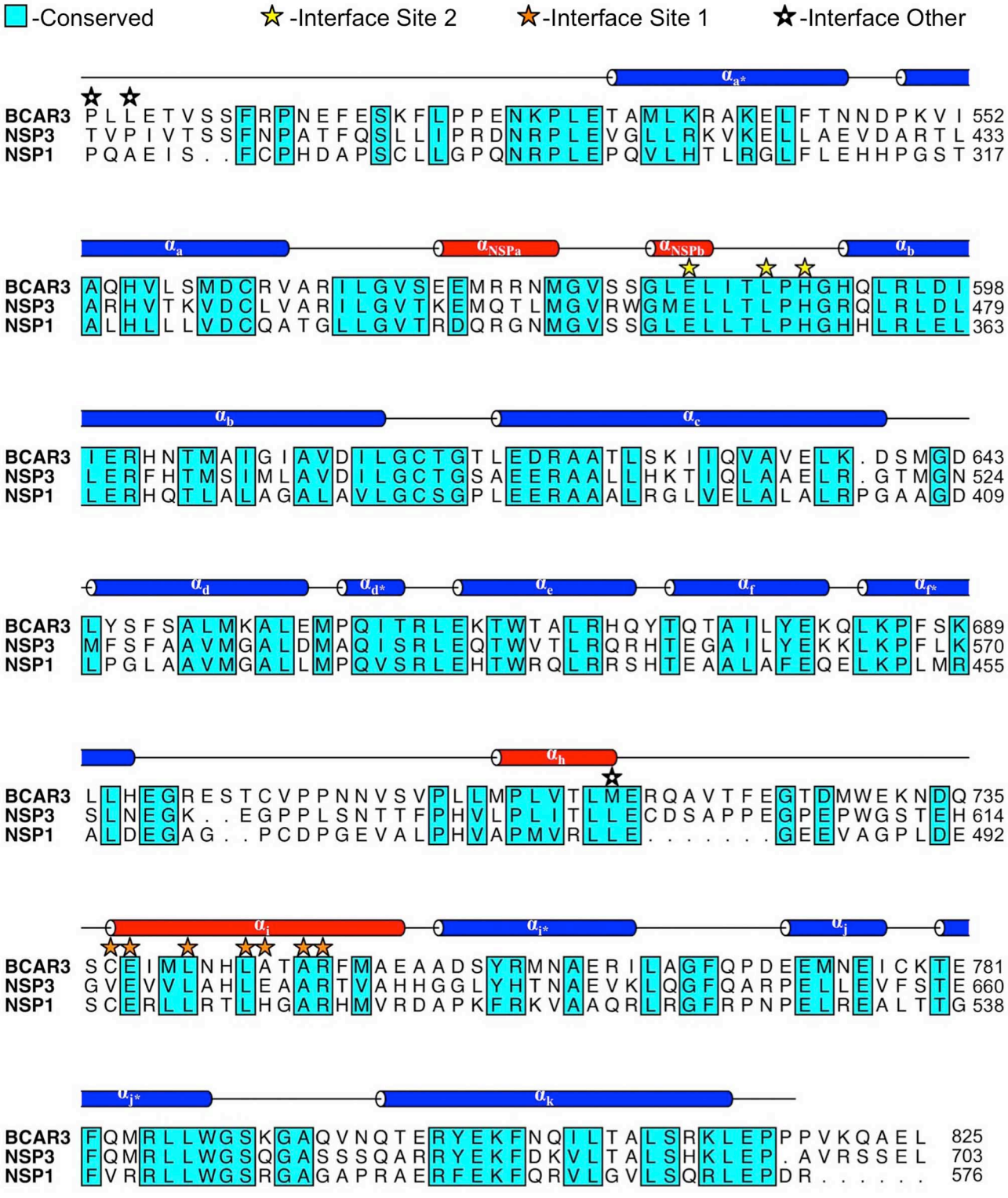

Supplementary Figure 8. continued. (b) Conservation of Cas-binding residues in NSP Cdc25-homology domains. Sequence alignment of the Cdc25-homology domains of NSP family proteins. Secondary structure elements of the BCAR3 Cdc25-homology domain are indicated as shown in **Supplementary Fig. 2**. Conserved residues are highlighted in cyan. Key residues for Cas interaction (based on the NSP3-p130Cas complex structure schematically shown in **Fig. 4a**) are denoted with stars and additionally colored orange for residues participating in Site 1 interactions and yellow for Site 2 interacting residues.